Measurement of R_2' in the Presence of Multiple Spectral Components Using Reference Spectrum Deconvolution[1]

F. W. Wehrli, J. Ma,[2] J. A. Hopkins, and H. K. Song

Department of Radiology, University of Pennsylvania Medical Center, Philadelphia, Pennsylvania

A method is described for measuring R_2', the RF reversible contribution to the effective transverse relaxation rate in yellow trabecular marrow, as a means to evaluate trabecular bone structure and density. The method exploits the similarity in spectral composition of the marrow and fat in subcutaneous tissue. Under these conditions the gradient echo envelope of the marrow signal can be regarded as a convolution of a function describing the bone marrow intravoxel line broadening (R_2') with a function expressing chemical shift modulation, which is obtained from the echo envelope of the subcutaneous fat signal in a reference region. Simple division of each of a series of echoes by the reference signal is shown to afford a smooth decay which can be fitted to a model to extract R_2'. The method has been evaluated in the upper femur of test subjects and a strong correlation of the thus derived R_2' values with those obtained by the GESFIDE technique is demonstrated. The close correspondence in spectral composition of proximal femur marrow and subcutaneous fat is further illustrated by means of localized spectroscopy. The major potential error source is global inhomogeneity in the reference region which can lead to an underestimation of the demodulation-derived R_2'. © 1998 Academic Press

Key Words: MRI; relaxation; bone marrow; trabecular bone.

INTRODUCTION

The reversible contribution, R_2', to the effective transverse relaxation rate, R_2^*, in trabecular bone marrow is related to the volume fraction (*1*) and orientation of the trabeculae (*2–4*). However, the measurement of R_2' is complicated by chemical shift modulation arising from the presence of multiple spectral components (*5*). For two-component systems the modulation can be removed by sampling at the chemical shift difference frequency (*6, 7*). Alternatively, one of the spectral components can be suppressed (*1*). At many skeletal sites, in particular in the adult appendicular skeleton, the marrow is entirely fatty. The spectrum of fatty acid triglyceride (FATG), the main constituent of yellow (fatty) marrow, has multiple spectral components which give rise to a complex modulation pattern (*8*). The problem is exacerbated by

the different R_2 ($=1/T_2$) relaxation rates of the various protons in FATG, which can cause errors in R_2' obtained by means of the GESFIDE technique (*7*). For example, the methylene protons α to the carboxyl group experience less segmental motion and therefore relax faster, thus causing multiexponential R_2 decay. Further, some of the modulations have long periods (on the order of a typical sampling period of the interferogram); therefore the apparent R_2^* and R_2' values will depend on the duration of the echo train.

In this paper a simple method for extracting R_2' is proposed that effectively removes the signal modulation by deconvolution with a reference signal collected in the same scan from adipose tissue in which line broadening due to local susceptibility variations is negligible. Unlike GESFIDE (gradient-echo sampling of FID and echo), this method thus circumvents a measurement of R_2, and its only requirement is that the chemical composition of the tissue used for the reference signal equals that in bone marrow and that global inhomogeneity across the imaging voxel is either negligible or similar to that in the ROI. The method was evaluated in the proximal femur *in vivo,* and the extracted R_2' values were compared with those obtained using the GESFIDE technique.

THEORY AND PRINCIPLE OF ANALYSIS

In the static dephasing regime where diffusional effects on transverse relaxation are negligible (*9*), the modulus gradient-echo signal $S(t)$ of an intrinsically inhomogeneous tissue such as trabecular bone marrow can be written as a product of two functions $f(t)$ and $g(t)$:

$$S(t) = f(t) \cdot g(t). \qquad [1]$$

In Eq. [1] $f(t)$ describes the amplitude modulations from chemical shifts and R_2 relaxation, and $g(t)$ accounts for signal attenuation from subvoxel susceptibility dephasing due to the presence of the diamagnetic bone trabeculae. It is fair to treat the marrow as a homogeneous mixture of its constituents, in which case water–fat susceptibility boundary effects are negligible, and thus in the absence of bone

$R_2' \approx 0$ for marrow. The function $g(t)$ is the Fourier transform of intravoxel field distributions, which in many magnetically inhomogeneous systems can be approximated by an exponential (i.e., $g(t) = A \exp(-R_2't)$) for which there is both theoretical (9) and experimental evidence (2).

The signal $S(t)$ in Eq. [1] has the properties of an interferogram (5, 10) and accounts for modulations by various spectral components (e.g., chemically shifted methylene, methyl, and olefinic protons in FATG) and their intrinsic relaxation. In general we can write for $S(t)$

$$S(t) = |\sum_k I_k e^{i\varphi_k} e^{-R_{2k}^* t}| = e^{-R_2' t} |\sum_k I_k e^{i\varphi_k} e^{-R_{2k} t}|, \quad [2]$$

where I_k is the initial amplitude of the kth spectral component; ω_k and $\varphi_k = (\omega_k + \Delta\omega)t$ represent its frequency and phase, respectively, of this component; and $\Delta\omega$ is a resonance offset, arising from global magnetic field inhomogeneity (on a scale much greater than the voxel size). As implied by Eq. [2] it can in general be assumed that the broadening from intrinsic field inhomogeneity (e.g., imparted by induced fields in the intertrabecular spaces) equally affects all spectral components, as expressed by the damping term $e^{-R_2't}$ outside the summation. We can rewrite Eq. [2] as

$$S(t) = e^{-R_2' t} [\sum_k \sum_l I_k e^{-R_{2k} t} I_l e^{-R_{2l} t} \cos[(\omega_k - \omega_l)t]]^{1/2}.$$

$$[3]$$

Summation in Eq. [3] is over all spectral components. It is to be noted that the interferogram is independent of a pixel-location-dependent resonance offset $\Delta\omega$. The argument of the cosine terms corresponds to the phase accumulated from the chemical shift differences between resonances k and l. The central hypothesis underlying the proposed method is that the subcutaneous fat has the same spectral composition except, of course, that there is no spectral broadening from R_2' effects since the tissue is magnetically homogeneous:

$$f(t) = [\sum_k \sum_l I_k e^{-R_{2k} t} I_l e^{-R_{2l} t} \cos[(\omega_k - \omega_l)t]]^{1/2}. \quad [4]$$

Therefore, the subcutaneous fat signal may serve as a reference signal to obtain the line broadening function. Measurements of both $S(t)$ and $f(t)$, therefore, permit determination of $g(t) = \exp(-R_2't)$ and thus R_2'. Note that the frequency domain counterpart of Eq. [1] corresponds to a convolution of the spectrum $F(\omega)$ with a line broadening function $G(\omega)$.

In most of the adult appendicular skeleton such as femur, marrow is of the yellow type, corresponding to about 85% by weight fat (11). Likewise, the principal tissue constituent in subcutaneous tissue is fat. Further, it is known that FATG composition of subcutaneous tissue and yellow bone marrow is nearly identical (ca. 30% saturated, 50% monounsatu-

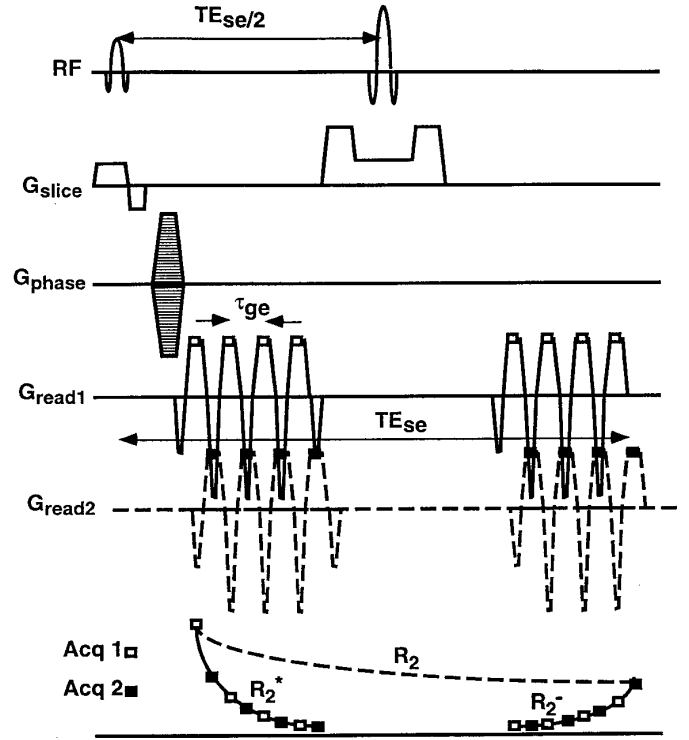**FIG. 1.** IMA-GESFIDE (interleaved multiple-acquisition GESFIDE) pulse sequence for measuring R_2' provides increased sampling frequency for sampling the signal envelope. Two interleaves offset by $\tau_{ge}/2$ are shown. The signals before and after the 180° RF pulse evolve with rate constants $R_2^* = R_2 + R_2'$ and $R_2^- = R_2 - R_2'$, respectively.

rated, and 20% polyunsaturated) (11), therefore resulting in very similar proton spectra. We shall demonstrate experimentally that this is indeed the case. We can further safely assume that T_1 (and T_2) in the reference region is the same as in the marrow region since fat in both instances arises from adipocytes; i.e., the cellular make-up is the same at both locations. Differential saturation, which could constitute a source of error, is thus not a concern. In these circumstances the chemical shift modulation is the same for the two tissues, except for a spin-density-dependent scaling factor k, i.e., $f_{sub}(t) = kf_{mar}(t)$. In this case $S(t)$ can be deconvolved through the operation

$$g_{mar}(t) = S_{mar}(t) \cdot kf_{sub}(t)^{-1}. \quad [5]$$

The knowledge of k is not relevant since it does not affect R_2'. Fitting $g_{mar}(t)$ to an exponential on a pixel basis thus allows determination of R_2' for trabecular bone marrow in the proximal femur as well as at other skeletal sites where marrow is fatty and the bone is trabecular (e.g., calcaneus, distal radius).

MATERIALS AND METHODS

In order to demonstrate the similarity in the spectral make-up of subcutaneous fat and bone marrow in the upper femur
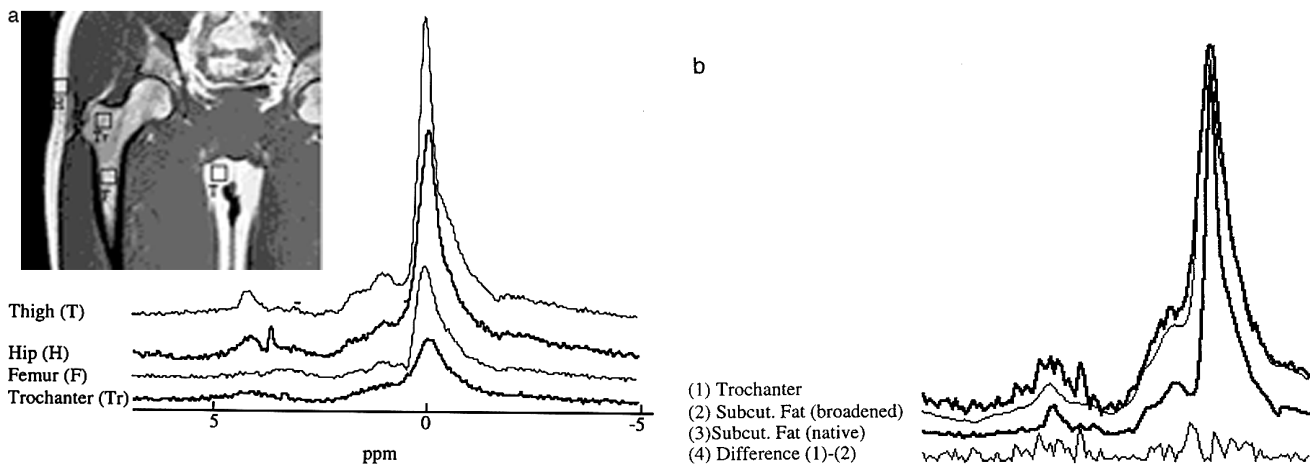
FIG. 2. Similarity of spectral composition in femoral bone marrow and subcutaneous fat: (a) Spectra from the four regions indicated in the inset localizer image illustrate the close similarity in spectral composition between the bone marrow in the upper femur and subcutaneous tissue used for reference spectrum deconvolution. Spectra are displayed on the same scale; lower amplitudes of the marrow spectra are a consequence of susceptibility-induced line broadening. Peaks are referenced to the methylene fatty acid reference. The least-shielded protons are due to the unsaturated fatty acid protons. Signals approximately 0.5 and 1 ppm downfield of CH_2 resonances pertain to protons α to carboxyl and allylic protons. (b) The exponentially broadened spectrum of subcutaneous fat (trace 3) subtracted from the spectrum of the trochanteric region (1) yields negligible residual (4).

in the adult skeleton, single-voxel PRESS (point-resolved spectroscopy (12)) spectra were obtained at four locations, representative of the two tissue types. Spectra, prescribed in the coronal plane, were collected on a 1.5-T General Electric Signa system operating in 5.6 configuration and using the commercial body RF coil. Voxel size was $1 \times 1 \times 0.5$ cm, TR and TE were 3.56 s and 35 ms, respectively, spectral width was 750 Hz, and 2048 data points were sampled with 32 signal averages.

Imaging was performed on a similarly configured 1.5 T GE Signa except that this latter was equipped with experimental 23 mT/m whole-body gradients with 230 T m^{-1} s^{-1} slew rate. For the measurements an interleaved version of GESFIDE was used (denoted ''IMA-GESFIDE''), which is depicted in Fig. 1. The basic GESFIDE principle has been described previously (7). In brief, two trains of gradient echoes, separated by a 180° pulse, sample the descending and ascending branches of the signal, which evolve with rate constants $R_2^* = R_2 + R_2'$, and $R_2^- = R_2 - R_2'$, respectively, from which R_2 and R_2' can be computed. The minimal sampling dwell time (time interval between successive echoes, τ_{ge}) is governed by the receiver bandwidth, the number of frequency-encoding samples, and gradient slew rate. By collecting the data in multiple interleaves the effective interecho time can be reduced and thus the measurement precision increased. Typically, two interleaves were used, resulting in 32 gradient echoes of 2.3 ms interecho spacing. Sixteen echoes preceded and 16 echoes followed the phase reversal RF pulse, with echo times ranging from 9.2 to 43.7 ms and 62.5 to 97 ms; TR was 500 ms and TE_{se} 97 ms. The image plane was coronal, and data were collected from three loca-

tions, with the center slice centered on the femoral head by means of an axial localizer image. The field of view and slice thickness were 38 cm and 5 mm, respectively, and 128 samples were collected in phase and frequency-encoding directions, affording a voxel size of $3.0 \times 3.0 \times 5$ mm. The rationale for the choice of the effective sampling interval of 2.3 ms was to probe the composition of bone marrow along with a measurement of R_2' in a clinical study of postmenopausal osteoporosis (13) by means of multipoint Dixon processing (14, 15) in a clinical study of the vertebrae.

In addition, R_2' was evaluated by interferogram deconvolution, as described above, using the FID portion of the GESFIDE data. For this purpose, a reference region was selected in the subcutaneous fat on the lateral side of the upper thigh, and $g_{mar}(t)$ computed pixel by pixel from Eq. [5]. Finally, to evaluate the spectral deconvolution method's precision and agreement with GESFIDE-derived R_2' values, R_2' was measured repeatedly in the same subject and subsequently in four volunteers.

All image processing was performed on either a Starmax 3000 desktop computer (MacOS 7.5.3) or a SUN 10/40 workstation, using IDL (Interactive Data Language, Research Systems, Inc., Boulder, CO). Raw data from the scanner were transferred to the SUN workstation, and Fourier transformed. The program was designed to output the following computed images: resonance offset $\Delta\omega$, R_2^*, R_2, $R_{2\,ges}'$ (obtained by GESFIDE processing), $R_{2\,dec}'$ (R_2' obtained by spectral deconvolution), fat, water, $r_{R_2^*}^2$ and $r_{R_{2\,dec}'}^2$ (maps of the square of the correlation coefficient for the fit of the gradient-echo signal (rate constant R_2^*) and for the same signal after deconvolution with the subcutaneous fat reference signal ($R_{2\,dec}'$)).
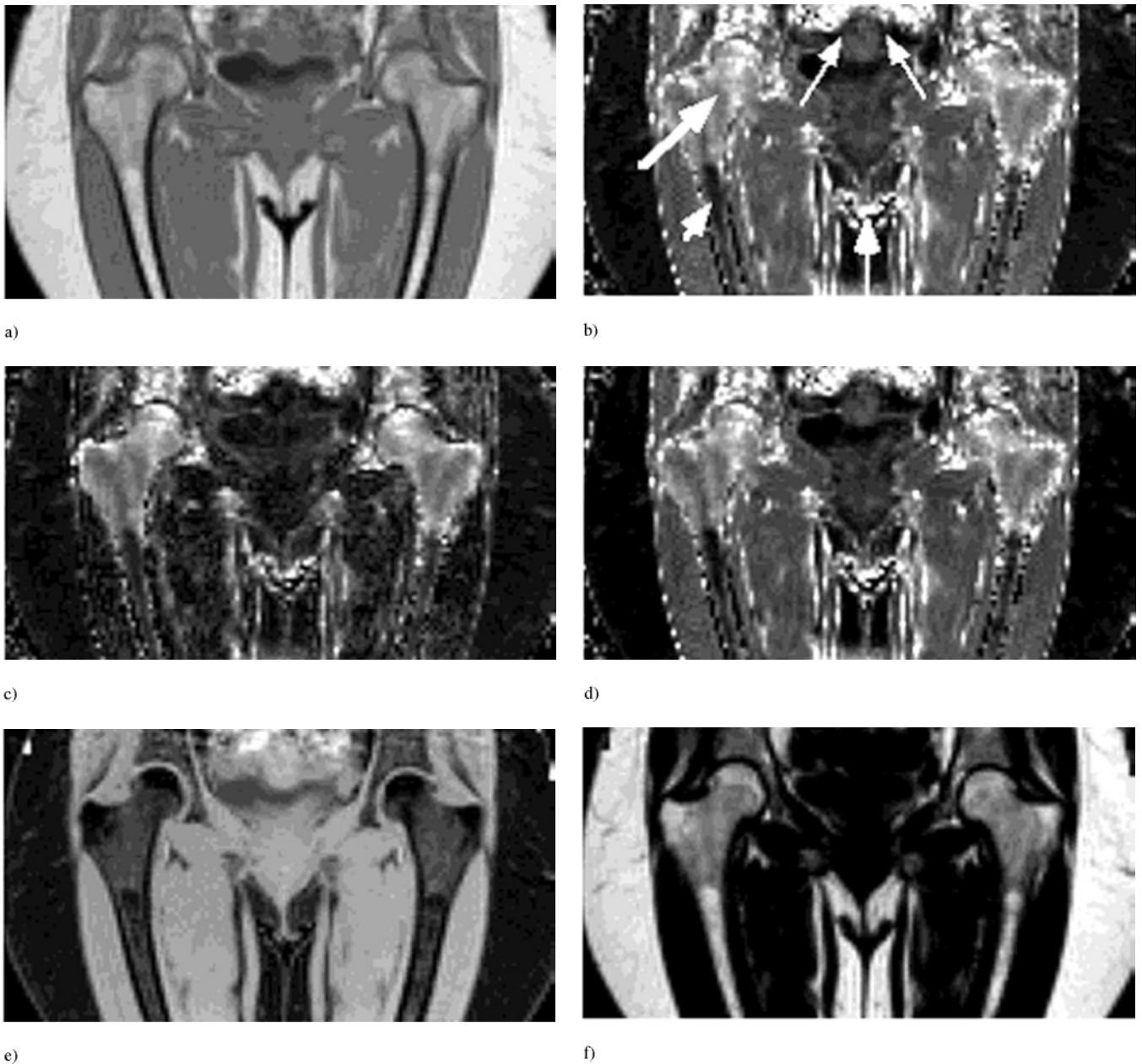
FIG. 3. Sample images obtained from IMA-GESFIDE acquisition: (a) first of a series of multiple gradient echoes; (b–f) computed images: (b) R_2^*, (c) $R'_{2\,\text{ges}}$ (GESFIDE-derived R'_2), (d) $R'_{2\,\text{dec}}$ (reference signal deconvolution derived image), (e) water, (f) fat image. The computed R_2^* and R'_2 maps (b–d) all exhibit strong enhancement in regions of high intrinsic field inhomogeneity, notably the upper femur (large arrow) which is rich in trabecular bone. By contrast, the femoral shaft and lower femur (arrow head) exhibit low intensity, i.e., low R_2^* and R'_2, commensurate with the absence of field-inducing trabeculae. Areas where magnetic field perturbations occur, such as air–tissue boundaries near the gut or inner thigh, are also enhanced (small arrows). Note the disparate behavior of the soft tissue signal in the R'_2 images in (c, d). Whereas homogeneous tissues such as subcutaneous fat and muscle have low R'_2 ($5–10\ \text{s}^{-1}$) as shown in the $R'_{2\,\text{ges}}$ image (c), muscle appears with artifactually high intensity in the $R'_{2\,\text{dec}}$ image (d). For details see text.

Since the spectral deconvolution method is sensitive to field inhomogeneity in the reference region, the choice of the subcutaneous fat ROI is critical. A search algorithm was designed to evaluate the relative inhomogeneity in fat. For this purpose fat pixels were first identified on the basis of the fat component images. A 3×3 averaging filter was then applied to the source images for pixels identified as subcutaneous fat. Finally, R_2^* was calculated for each 3×3 pixel ROI

by fitting the interferogram to a decaying exponential, and the ROI of minimum R_2^* selected for deconvolution.

Finally, the sensitivity of the apparent R_2' to spectral mismatch between target and reference region was examined by simulation. For this purpose a synthetic spectrum was generated that duplicated the subcutaneous reference spectrum. This spectrum was broadened to correspond to an R_2' value as it is typically encountered in trabecular bone marrow. In order to simulate the effect of contamination of the fatty bone marrow with a hematopoietic constituent, water was gradually added to the spectrum and an interferogram computed according to Eq. [3] which was deconvolved with the reference interferogram to yield an apparent R_2' ($R_{2\,\mathrm{app}}'$). The error in measured R_2' was expressed in percent error from the true value, $100 \times (R_{2\,\mathrm{app}}' - R_2')/R_2'$, and plotted versus the percent of water spins in the marrow region.

RESULTS

Figure 2a shows spectra obtained in a 27-year-old male subject at the four skeletal locations indicated in the accompanying localizer image. The spectra demonstrate the predominantly fatty marrow in the upper femur and the similarity in the spectral make-up between these locations and typical reference regions in subcutaneous fat. Further evidence of the close similarity in spectral composition between the subcutaneous reference region and the trabecular bone marrow in the upper femur is provided in Fig. 2b, which shows spectra of the trochanteric region, the subcutaneous fat, and the latter exponentially broadened. The difference spectrum of the marrow and broadened fat spectrum exhibits negligible residual.

Figure 3 displays a source image along with the most relevant computed images. The R_2^* image (Fig. 3b) emphasizes regions of high intrinsic field inhomogeneity, notably trabecular bone in the upper femur and acetabulum. Muscle also is relatively bright by virtue of its large R_2 (~ 35 s^{-1}). Figure 3c shows an R_2' map obtained by GESFIDE processing ($R_{2\,\mathrm{ges}}'$). Besides some regions that are enhanced by global inhomogeneity caused, for example, by air in the gut, all magnetically homogeneous tissues (muscle, subcutaneous fat) appear with near background intensity. By contrast trabecular bone, which has large R_2' (20–80 s^{-1}, depending on trabecular density and orientation) is enhanced. The R_2' map derived by reference signal deconvolution ($R_{2\,\mathrm{dec}}'$) in Fig. 3d is similar in appearance except for the soft tissues. Muscle appears bright and is almost identical in intensity to that of the R_2^* image. This discrepant behavior of the two types of R_2' images is readily understood when considering that the deconvolution process only removes the very small line broadening in subcutaneous fat ($R_2' \sim$ 5–10 s^{-1}). Therefore, the signal pertaining to muscle is dominated by R_2, and regions in $R_{2\,\mathrm{dec}}'$ images outside fatty trabecular bone marrow are thus not relevant.
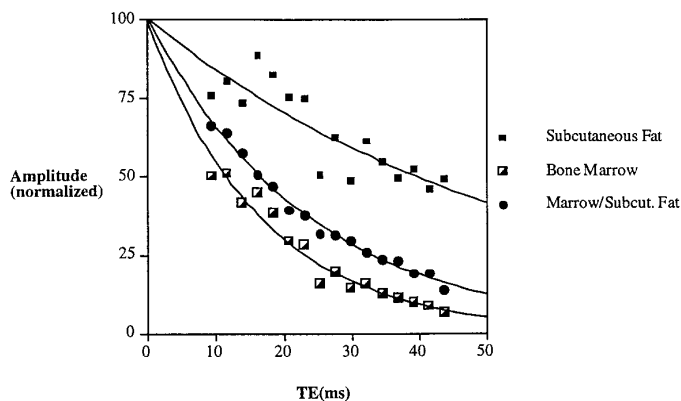

FIG. 4. Plot of ROI signal amplitude measured from 16 gradient echoes, normalized so that initial amplitudes are equal. Strong chemical shift modulation of the subcutaneous fat signal (top trace) is noted, which also occurs in the bone marrow of the greater trochanter of the femur (bottom trace). A smooth curve which fits to an exponential ($R^2 = 0.985$) is obtained by dividing marrow/subcutaneous fat, thus demonstrating the effectiveness of the demodulation (center trace).

In Fig. 4 ROI signal amplitudes taken in subcutaneous fat and the trochanter of the proximal femur are plotted vs gradient-echo time. Note the strong modulation caused by FATG spectral modulation. Deconvolution with a reference signal derived from subcutaneous fat has the effect of demodulating the signal, resulting in a smoothly decaying exponential evolving with rate constant R_2'. The hypothesis that the chemical composition of the subcutaneous fat is similar to that of the bone marrow in femur is borne out by the similar temporal modulation of the signal which was found in all subjects studied.

The sensitivity of the derived R_2' values to spectral mismatch between marrow and reference region was evaluated as described under Materials and Methods. Whereas in the adult appendicular skeleton the marrow is almost exclusively fatty (16) this is not the case in the vertebrae, for example, and the technique would thus not be applicable to the spine. Nevertheless, even in the femur small deviations from an all-fatty marrow make-up may occur. Therefore, the error incurred as a result of replacement of fat by water in the marrow region is of some interest. Figure 5 shows the resulting error in apparent R_2' as a function of added water for three typical R_2' values. The error is found to scale almost linearly with water concentration and is negative, thus leading to an underestimation of R_2'. Further, its magnitude increases with decreasing R_2'.

Figure 6 shows a correlation between R_2' obtained by the two different methods (GESFIDE vs the current deconvolution method) in four subjects for various ROIs. The large range of values reflects the widely varying trabecular density in the ROIs chosen. The R_2' map of Fig. 6a indicates very low density in the femoral shaft and Ward's triangle, intermediate density in the greater trochanter, and very high den-
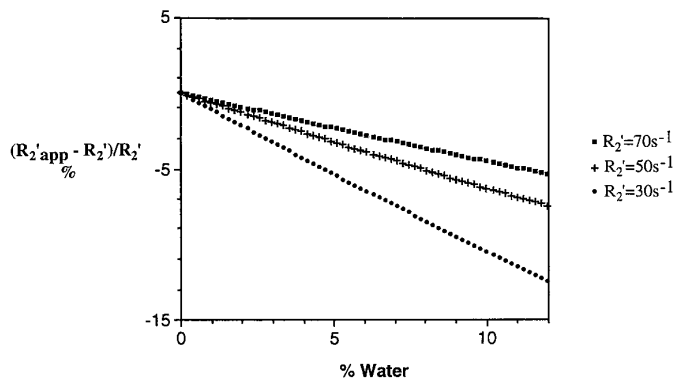
FIG. 5. Error in apparent R_2' derived by deconvolution of the fatty marrow interferogram with a reference waveform obtained by gradual addition of water (in volume %) while decrementing the fat fraction. For the calculation, $T_{2,\text{water}} = 35$ ms was assumed.

TABLE 1
Results of Reproducibility Evaluation

Parameter	Intrasession ($n = 3$)			Intersession ($n = 3$)		
	Mean	Std. dev.	c.v.	Mean	Std. dev.	c.v.
R_2^*	69.6	0.6	0.9	69.2	1.6	2.4
R_2	12.4	0.6	5.1	12.7	0.1	0.6
$R_{2\text{ges}}'$	57.1	0.1	0.1	56.4	1.6	2.8
$R_{2\text{dec}}'$	52.10	1.16	2.2	51.7	0.8	1.6

Note. Intrasession refers to repeat measurements in the same subject within a single imaging session, intersession involved repeat measurements in the same subject in successive imaging sessions. All data are in reciprocal seconds (s^{-1}) except coefficient of variation (c.v.) which is in percent. $R_{2\text{ges}}'$ and $R_{2\text{dec}}'$ refer to R_2' values derived by GESFIDE and reference signal deconvolution processing, respectively.

sity in the femoral head. The data indicate $R_{2\text{ dec}}'$ to be systematically lower than R_2' obtained by the GESFIDE method. The likely cause of this consistently observed trend is global inhomogeneity in the reference region. The deconvolution operation corresponds to a subtraction of the relaxation rate in the reference region from that in the analytical region (bone marrow). Hence, artifactual line broadening from macroscopic field inhomogeneity in the reference region causes an underestimation of R_2'. Another possible cause of this discrepancy is the presence of a small excess concentration of water in the marrow region which, as has been demonstrated, causes a reduction in the apparent R_2'.

Both methods are remarkably reproducible, as the data from repeat scans show (Table 1). ''Intrasession'' refers to measurements conducted by repeating the scans with the subject landmarked identically. By contrast, in the ''intersession'' study the subject was removed from the table between scans. The latter thus is a measure of serial reproducibility in longitudinal studies where the variance is primarily determined by failure to accurately match up the ROIs which is particularly critical in the femur where trabecular density (and structural organization) is highly variant. Nevertheless, a coefficient of variation of 3 and 1.5% for GESFIDE and deconvolution-derived R_2' is quite encouraging (though it is still inferior to dual-energy X-ray absorptiometry).

DISCUSSION AND CONCLUSIONS

The deconvolution method provides an efficient means for deriving R_2' of magnetically inhomogeneous tissues in the presence of multiple spectral components, on condition that a reference signal of identical spectral make-up be avail-
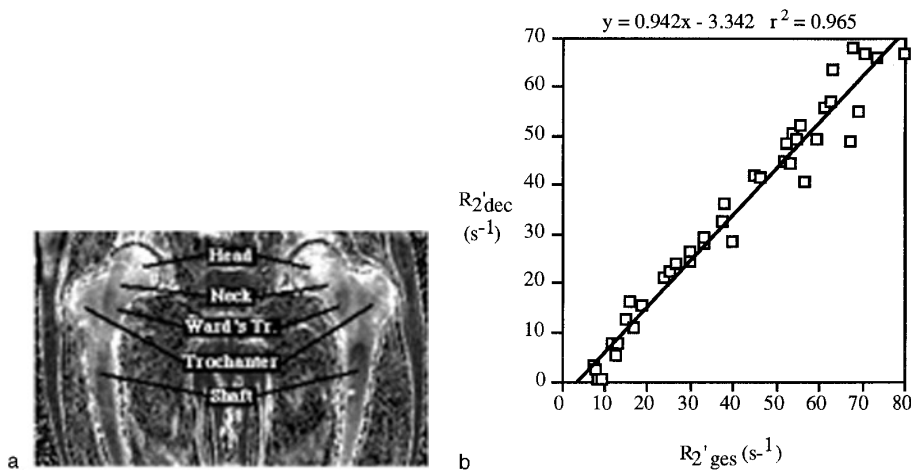

FIG. 6. Relationship between $R_{2\text{ dec}}'$ and $R_{2\text{ ges}}'$ (derived by GESFIDE processing). Data combined from four subjects using ROIs indicated in the R_2' image for both femurs (a); (b) $R_{2\text{ dec}}'$ computed by deconvolving 16-point interferogram with the modulus signal from ROI in subcutaneous fat and fitting residual to an exponential. Note that $R_{2\text{ dec}}'$ is systematically lower than R_2' derived by GESFIDE.

able and that this latter not be modulated by the field perturbers. The apparent R_2' or R_2^* relaxation rates obtained by the GESFIDE technique (or any method that fails to remove the chemical shift modulations, such as echo offset methods (*1*)) depend on the length of the echo train or range of echo offset increments. This is evident when considering the nature of modulations present in the rather complex FATG spectrum. Some of these modulations have periods of 30 ms and longer at 1.5 T (corresponding to chemical shift differences of 0.5 ppm such as the those between methylenes and α-carboxy (CH_2's) (*5*). By contrast, R_2' derived with the deconvolution method should be entirely independent of echo train length (ignoring, of course, the effect of noise). Processing is extremely simple in that it requires only division of each echo by the reference modulus signal. Another limitation of the GESFIDE and related methods is the assumption of monoexponential R_2 relaxation. However, the protons in the fatty acid chains have different effective correlation times. For instance, relaxation of protons closer to the glyceryl moiety relax faster, and thus their contribution to the echo decreases rapidly with increasing TE (for a discussion of segmental motion and their implications on relaxation rates, see, for example, Ref. (*17*)). This phenomenon manifests in an anomalously intense signal at very short TE, an observation which is very consistent and which prompted us to discard the TE = 4.6 ms echo for GESFIDE processing. By contrast, the nature of the modulation is irrelevant in the present method.

The major source of error is differences in background gradients (as arising from poor shimming or large-scale susceptibility effects) at the reference site, which are often present since the subcutaneous tissue is near tissue–air boundaries. In this case, as is readily seen, R_2' is underestimated. Searching for a reference region of optimum field homogeneity is relatively straightforward and should remedy the problem. The algorithm used for this purpose was found to provide fairly consistent R_2^* for the range of subjects studied. Obviously, the reverse is also possible in that the macroscopic field gradients in the analytical region (i.e., trabecular bone marrow) could exceed those in the reference region, in which case R_2' is overestimated. Such errors can in principle be corrected with a separate deconvolution since the field gradients are obtainable from the multiecho data (*15*). However, in practice this is more complicated since the largest voxel dimension is usually the one orthogonal to the imaging plane and thus artifactual dephasing due to background gradients in this direction is the greatest (*18*). The detrimental effects of the background gradients themselves can be minimized by decreasing voxel size. There are, of course, practical limits in doing so, not least because R_2' from subvoxel microscopic gradients (the quantity of interest) becomes itself voxel size dependent as voxel size decreases (*1*). Three-dimensional gradient-echo techniques minimize dephasing from macroscopic

background gradients (*19*) but these techniques would lead to considerably longer scan times and very large data arrays. Another potential difficulty is the lack of a suitable reference ROI in subjects with a thin subcutaneous layer. Finally, the method fails for mixed bone marrow such as in the vertebrae where the composition of the marrow is variably fatty/hematopoietic (*20*).

In summary, the spectral deconvolution method presented has likely applications for the evaluation of cancellous bone structure and density at anatomic sites of predominantly fatty marrow, which essentially comprises the entire appendicular skeleton. Its main benefit is the direct measurement it enables of R_2' with a minimum of processing, while circumventing the complications from chemical shift modulation, which hamper virtually all alternative methods. Finally, the method may gain additional significance in light of recent evidence suggesting that osteodensitometry may be more effective at sites of yellow marrow (*21*).

REFERENCES

1. S. Majumdar and H. K. Genant, In vivo relationship between marrow T_2^* and trabecular bone density determined with a chemical shift-selective asymmetric spin-echo sequence, *J. Magn. Reson. Imaging* **2**, 209–219 (1992).

2. H. Chung, F. W. Wehrli, J. L. Williams, and S. D. Kugelmass, Relationship between NMR transverse relaxation, trabecular bone architecture and strength, *Proc. Natl. Acad. Sci.* **90**, 10,250–10,254 (1993).

3. H. Chung and F. W. Wehrli, T_2^* and material anisotropy of cancellous bone, *in* Proceedings of the Society of Magnetic Resonance in Medicine 12th Annual Meeting, New York, Vol. 1, p. 138 (1993).

4. D. A. Yablonskiy, W. R. Reinus, E. M. Haacke, and H. Stark, Quantitation of T_2' anisotropic effects on MR bone mineral density measurement, *Magn. Reson. Med.* **37**, 214–221 (1996).

5. J. C. Ford and F. W. Wehrli, In-vivo quantitative characterization of trabecular bone by NMR interferometry and localized proton spectroscopy, *Magn. Reson. Med.* **17**, 543–551 (1991).

6. F. W. Wehrli, J. C. Ford, and J. G. Haddad, Osteoporosis: Clinical assessment with quantitative magnetic resonance imaging in diagnosis, *Radiology* **196**, 631–641 (1995).

7. J. Ma and F. W. Wehrli, Method for image-based measurement of the reversible and irreversible contribution to the transverse relaxation rate, *J. Magn. Reson. B* **111**, 61–69 (1996).

8. F. W. Wehrli, D. G. Perkins, A. Shimakawa, and F. Roberts, Chemical shift-induced amplitude modulations in images obtained with gradient refocusing, *Magn. Reson. Imaging* **5**, 157–158 (1987).

9. D. A. Yablonskiy and E. M. Haacke, Theory of NMR signal behavior in magnetically homogeneous tissues: The static dephasing regime, *Magn. Reson. Med.* **32**, 749–763 (1994).

10. F. W. Wehrli, Trabecular bone imaging, *in* ''Encyclopedia of Magnetic Resonance'' (D. M. Grant and R. K. Harris, Eds.), pp. 4803–4811, Wiley, New York (1995).

11. E. Zach and E. Shafrir, Composition of bone marrow adipose tissue in relation to body fat depots in various species, *Isr. J. Med. Sci.* **10**, 1541–1550 (1974).

12. P. Bottomley, Spatial localization in NMR spectroscopy in vivo, *Ann. NY Acad. Sci.* **508**, 333–348 (1987).

13. F. W. Wehrli, J. Ma, J. C. Ford, and J. G. Haddad, MR R_2' and DEXA bone densitometry in the normal and osteopenic proximal femur, *in* Proceedings of the International Society of Magnetic Resonance in Medicine, Fifth Annual Meeting, Vancouver, Vol. 1, p. 146 (1997).

14. G. H. Glover and E. Schneider, Three-point Dixon technique for true water/fat decomposition with B_0 inhomogeneity correction, *Magn. Reson. Med.* **18,** 371–383 (1991).

15. J. Ma, F. W. Wehrli, H. K. Song, and S. N. Hwang, A single-scan imaging technique for quantitation of the relative contents of fat and water protons and their transverse relaxation times, *J. Magn. Reson.* **125,** 92–101 (1997).

16. S. Trubowitz and S. Davis, Eds., ''The Bone Marrow Matrix,'' CRC, Boca Raton, FL (1982).

17. F. W. Wehrli, Organic structure assignments using C-13 spin–lattice relaxation data, *in* ''Topics in Carbon-13 NMR Spectroscopy'' (C. C. Levy, Ed.), Vol. 2, pp. 343–385, Wiley, New York (1976).

18. J. Frahm, K. D. Merboldt, and W. Hänicke, Direct FLASH imaging of magnetic field inhomogeneities by gradient compensation, *Magn. Reson. Med.* **6,** 474–480 (1988).

19. E. M. Haacke, J. A. Tkach, and T. B. Parrish, Reducing T_2^* dephasing in gradient field-echo imaging, *Radiology* **170,** 457–462 (1989).

20. F. Schick, H. Bongers, W. I. Jung, M. Skalej, O. Lutz, and C. D. Claussen, Volume-selective proton MRS in vertebral bodies, *Magn. Reson. Med.* **26,** 207–217 (1992).

21. J. Machann, F. Schick, D. Seitz, S. H. Duda, K. Straubinger, O. Lutz, and C. D. Claussen, Osteodensitometry in yellow and red bone marrow using magnetic resonance—Comparison with computed tomography, *in* Proceedings of the International Society of Magnetic Resonance in Medicine, 3rd Annual Meeting, New York, Vol. 2, p. 1093 (1996).